University of Bath

Alternative formats
If you require this document in an alternative format, please contact:
openaccess@bath.ac.uk

Bactericidal – Bacteriostatic Foam Filters for Air Treatment

Ramya G[a],*, Olivier Camus[a], Y. M. John Chew[a], Barry Crittenden[a] , Semali Perera[a],*

[a]Centre for Advanced Separations Engineering, Department of Chemical Engineering,

University of Bath, Claverton Down, Bath BA2 7AY, UK

Abstract

A highly loaded porous polyimide (PI) foam type air filter has been fabricated by incorporating antimicrobial active metals to prevent microbial growth and kill microbes, and so to provide health benefits for people in enclosed spaces. PI foams containing antibacterial agents such as PCu80 (PI (20 wt%)/copper (80 wt%)), PNi80 (PI (20 wt%)/nickel (80 wt%)) and copper – nickel composites were synthesized and tested against model bacterium, *Erwinia carotovora* (Gram-negative) to determine the anti-bacterial efficacy of the air filter. Scanning electron microscope – energy dispersive X-ray spectroscopy (SEM – EDX) confirmed the distribution of copper and nickel throughout PCu80 and PNi80 where concentrations between 70 and 75% were detected. The copper : nickel ratio was consistent throughout the foam for PCu64Ni16 (PI (20 wt%)/copper (64 wt%)/nickel (16 wt%)). PCu80 displayed a high log reduction value (LRV) of 99.996% and thus exhibited a bactericidal effect. PNi80 displayed a lower LRV of 99.4%. However, a higher LRV value was observed compared to the control, 95.5% (PI foam without antibacterial agent) and thus, demonstrated a bacteriostatic effect. PCu64Ni16 exhibited and sustained exceptional microbe removal efficiencies of 99.9997% for 24 hrs at high humidity levels and demonstrated the highest zone of inhibition (ZOI) value of 33.90 ± 0.16 mm compared to PCu80 (27.5 ± 1.1 mm). Nickel strongly inhibited the proliferation of bacteria whilst copper destroyed the bacteria on the foam filters. Therefore, such functionalized filters can potentially overcome the inherent limitation in conventional filters and imply their superiority for controlling indoor air quality.

1 Introduction

In recent years the urge to remove airborne microbes has led to a renewed interest in energy efficient filter media and techniques for air filtration in commercial, industrial and consumer sectors, especially in enclosed environments such as aircraft, automotive cabins, clean rooms and hospitals, where the absence of micro-organisms is essential. Generally, atmospheric air acts as a carrier for the circulation of microbial cells, dormant spores as well as fungi. Airborne contaminants such as microbiological particulates have become predominant factors when defining cabin or indoor air quality due to their effect on human health.[1,2] In applications such as cabin air filtration in aircrafts or indoor air clean up, state-of-the-art high-efficiency particulate air (HEPA) filters are being used. However, despite these filters being able to remove 99.99% of airborne particles, accumulation and proliferation of microbes, cost and routine maintenance are associated problems.[3,4] Moreover, the organic and particulate matter deposited on the filter medium contribute to microbial growth and they thrive in heating, ventilation and air-conditioning (HVAC) systems at the appropriate temperature and humidity environment.[5–7] A study conducted by the National Institute for Occupational Safety and Health (NIOSH) on 529 buildings reported that 53% of indoor air pollution was due to the HVAC system.[8]

Since HEPA filters cannot be reused, this results in additional costs due to regular replacement and maintenance. Unless the filter is functionalized with antimicrobial agents, the still-living microbes will continue to breed or reproduce in the filter. Although some antimicrobial metals such as sodium, magnesium, potassium, calcium, vanadium, chromium, manganese, iron, cobalt, nickel, copper, zinc, selenium and molybdenum are essential for the normal physiology and function of organisms, these metals become lethal to all cells when present in excess. There are also other metals such as silver, mercury and tellurium which are extremely poisonous to most bacteria and have microbiocidal activity at very low

3

concentrations.[9] Copper and silver are most frequently used due to their excellent antimicrobial properties against a variety of different micro-organisms and their efficacy in killing bacteria.[10–12] Since it is cheaper than silver, it is possible to incorporate high concentrations (>55%) of copper to achieve the required antibacterial activity.[13,14] Unlike copper, silver containing materials exhibit no antimicrobial efficacy at typical indoor conditions such as in hospitals.[15] Therefore, copper was selected as one of the model antibacterial agents in this study. Studies have shown that when antibacterial agents are used in combination, the antibacterial effect is greater compared to the effects of an individual agent.[16,17] Nickel was selected to be used in combination with copper due to its low cost as well as its bacteriostatic effect.[18]

A number of studies have reported the impregnation of antibacterial agents into structures such as polyurethane, silicon carbide foam, monoliths and electrospun nanofiber membranes for air filtration to inhibit growth of bacteria.[19–23] Vukčević et al.[19] performed a study on carbon monoliths impregnated with silver. The disadvantage of the monolithic structure is its lack of tortuosity compared to the HEPA filter. This reduces the efficiency of the monolith in being able to trap and kill the bacteria. Additionally, the rate of silver deposition onto the monolith surface is a very slow process. Lv et al.[20] reviewed the advantages and disadvantages of green electrospinning for various applications in their paper. Zhu et al.[21] and Lv et al.[22] used a thermo – curing electrospinning process to prepare electrospun nanofiber membranes incorporated with silver and zinc oxide nanoparticles respectively. Although the nanofibre membranes provide the tortuosity effect observed in HEPA filters for trapping and killing bacteria, membrane fouling as well as the rate of production of defect free fiber membranes via the electrospinning process may be challenging. Paladini et al.[23] prepared a silver coated polyurethane foam by placing it in a silver nitrate solution and exposing it to UV radiation to induce the synthesis of silver nanoparticles. The disadvantage of polyurethane is that it cannot

be heated up to temperatures greater than 150°C for reuse. In addition, producing these foams on a large scale would require large quantities of silver and thereby incur high material costs. Hu et al.[24] prepared a ZnO coated SiC foam by soaking the substrate in zinc solution and calcining it at 500 – 800°C in air. Calcination requires a substantial amount of heating to achieve such high temperatures and thus manufacturing costs increase. Kim et al.[25] achieved a copper content of up to 60 wt% by forming a slurry in a polymer latex medium to allow impregnation of the particles into a polyurethane foam. However, this polyurethane foam was used to combat arthritis and rheumatism by coming into direct contact with the patient's skin. In order for antibacterial foam filters to be active, the polymer should not cover the active agents, the filter should have a highly porous structure for exposure of the antibacterial metals to the microbes, the polymer binder should be thermally and mechanically stable, and the filter should ideally be reusable.

Ceramic foams are suitable for high temperature, abrasive and severely corrosive environments due to their high thermal and chemical stability.[26] However, their manufacture requires high temperatures ranging from 1400°C to 1600°C for a sintering process to produce a ceramic skeleton.[27,28] This paper presents the manufacturing of polymeric foams incorporated with antibacterial agents at room temperature via a simple process involving two reactions occurring simultaneously namely, 'blowing' and polymerization.[29,30] Polyimide (PI) was selected for this study as it is commercially used due to its high mechanical strength and thermal stability, owing to the presence of heterocyclic units in the polymeric structure.[31] Although *Erwinia carotovora* is a plant pathogenic bacterium which causes soft rot and blackleg disease of fruits and vegetables, it is a Gram negative bacterium[32] and it was selected as a model micro-organism as it has similar transport proteins as other Gram-negative bacteria such as the more commonly used *Escherichia coli* because both types of bacteria are from the same

5

Enterobacteriaceae family.[33] In addition, not only is it safe for use in a university based laboratory, it also has a fast doubling time of 43 ± 2 min.[34]

This paper presents the development and evaluation of copper, nickel and copper – nickel encapsulated PI foam structures which exhibit bactericidal and bacteriostatic properties for the removal of airborne microbes. The distribution of copper, nickel and copper – nickel throughout the foams was confirmed using scanning electron microscope – energy dispersive X-ray spectroscopy (SEM – EDX). The antibacterial efficacy of the copper, nickel and copper – nickel composite foams when challenged with a bacterial (*Erwinia carotovora*) aerosol was assessed by using staining methods, log reduction values and zone of inhibition tests.

2   *Materials and Methods*

2.1   Materials

Pyromellitic dianhydride (97%) (PMDA), 1-methyl-2-pyrrolidone (Reagent grade, 99%) (NMP), silicon oil (viscosity 350 cSt), triethanolamine (Amine Catalyst), dibutyltin dilaurate (Tin Catalyst), poly [(phenyl isocyanate)-co-formaldehyde] (Isocyanate) and copper (powder, <75 μm, 99%) were sourced from Sigma-Aldrich. Nickel (Flake grade HCA-1, ~ 1 μm, >99.8%,) was sourced from Hart Chemicals. LB Broth, Miller for growth media preparation and LB Agar, Miller for agar plate preparation were purchased from Fisher Scientific. *Erwinia carotovora* was sourced from the Department of Biology and Biochemistry at University of Bath.

2.2   Preparation of Copper, Nickel and Copper – Nickel Composite Foams

PMDA (5 g), NMP (40 – 45 mL), distilled water (2 – 5 mL), amine catalyst (~50 μL), silicon oil (1 – 2 g) were mixed using a homogenizer at 6500 rpm for 30 seconds to give a first mixture. Copper (40 g) and tin catalyst (~25 μL) were added to the first mixture and stirred using a homogenizer at 6500 rpm for 30 seconds to give a second mixture. The second mixture and

5 g of isocyanate were mixed using the homogenizer at 6500 rpm for 5 seconds. The formulation for fabricating the copper, nickel and copper – nickel composite foams was adapted from G et al.[35] and extensive modifications were made to the recipe. The water content and amount of solvent etc. have been carefully considered because it is critical that the foam should be able to support the weight of the antibacterial agents as well as consist of an open-cell porous structure. The PI foam containing the antibacterial agents was synthesized via a simultaneous 'blowing' and polymerization reaction. The detailed reaction chemistry has been explained in G et al.[35] The resulting foam was soaked in a water bath overnight and dried in an oven at 100°C till no change in foam weight was observed. This process was used also for preparing PI/nickel (80 wt%) foams as well as PI/copper – nickel composite foams. This can be seen in Table 1.

Table 1. Antibacterial polyimide foam samples with varying compositions[a].

Anti-bacterial Foam	Copper Content	Nickel Content	PI Content	Sample Name
PI/copper	80 wt%			PCu80
PI/nickel		80 wt%		PNi80
PI/copper – nickel	16 wt%	64 wt%	20 wt%	PCu16Ni64
PI/copper – nickel	32 wt%	48 wt%		PCu32Ni48
PI/copper – nickel	48 wt%	32 wt%		PCu48Ni32
PI/copper – nickel	64 wt%	16 wt%		PCu64Ni16

[a]P indicates polyimide, Cu indicates copper and Ni indicates nickel

The densities of the composite foams were determined by dividing the mass of the foams by its' volume. The porosities of the foams were calculated using a saturation method.[36]

2.3 Antibacterial Experiment

Antibacterial experiments were carried out to determine the efficacy of PI/copper, PI/nickel and PI/copper – nickel foams. Figure 1 shows the antibacterial rig which consists of a feed gas flow system, a module containing the antibacterial foam and a collision 3-Jet MRE type

nebulizer which generates a bacterial aerosol. The rotameter regulates the air flowrate at 1 L min^{-1} and is bubbled through the bacterial solution. The generated bacterial aerosol passes through the tubular module containing the antibacterial foam. Bacteria present in the outlet stream are trapped by the filter paper as shown in Figure 1. The outlet stream from the module then passes into bleach solution.
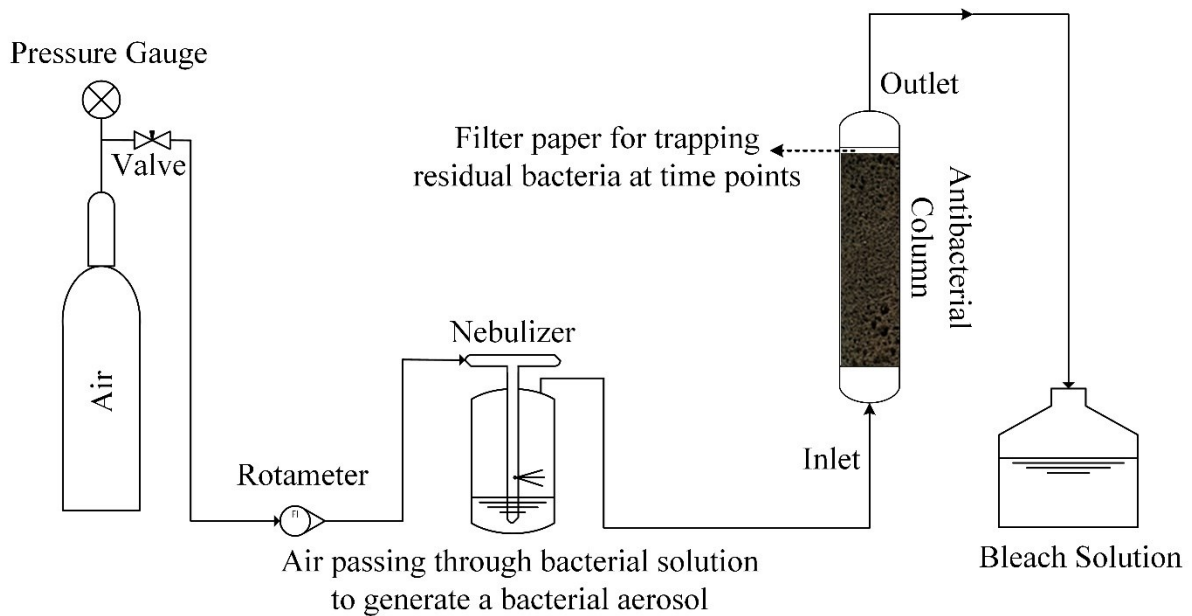

Figure 1. Schematic of the anti-bacterial rig.

The bacterial solution was prepared by inoculating growth media (100 mL) with the bacteria, *Erwinia carotovora* and incubated overnight at 25°C. Prior to the experiment, the optical density (OD) of the bacterial solution is adjusted to 1 using growth media so as to ensure that the concentration of bacteria passing through the different foam filters is consistent. The time points at which the filter paper is removed and replaced are 15 min, 30 min, 1 hour, 2 hours, 4 hours, 6 hours and 24 hours. The removed filter papers are rinsed in a vial containing distilled water (2.5 mL). The bacterial water (100 μL) from the vial is plated onto an agar plate and incubated at 25°C for 24 hours. This was repeated for all time points. At the end of the experiment, the foam filters were soaked in bleach solution and placed in an autoclave

(Temperature: 120°C, Pressure: 2 bar) for further sterilisation of the foams. The foams were then placed in a 120°C oven to dry the foams. Blank tests were first carried out for 15 min to determine the number of bacterial colonies flowing through the empty tubular module. The blank tests gave an average value of 246500 ± 2.6% colonies in 15 min. The antibacterial activity of the foams was determined using eq 1 (adapted from BS ISO 22196:2011[37]) to calculate log reduction values (LRVs).

$$LRVs = log \frac{(Initial\ estimated\ bacterial\ count\ for\ each\ time\ point\ based\ on\ blank\ test)}{(Bacterial\ count\ at\ foam\ outlet\ at\ each\ time\ point)} \qquad (1)$$

LRVs signify the reduction in bacterial colonies observed when the foam filter is compared to the blank test. The reduction in bacterial colonies can be presented in the form of log values (1-Log, 2-Log, 3-Log, etc.) as well as in the form of a percentage (90%, 99%, 99.9%, etc.). 1-Log is equivalent to 90% due to a 10-fold reduction of colonies, 2-Log is equivalent to 99% due to a 100-fold reduction of colonies, 3-Log is equivalent to 99.9% due to a 1000-fold reduction of colonies and so on.

2.4 Zone of Inhibition (ZOI) Test

ZOI tests were done for the prepared antibacterial foam samples according to the 2019 guidelines of the European Committee of Antimicrobial Susceptibility Testing (EUCAST).[38] 90 mm circular plates containing agar medium of approximately 4.0 mm in height were prepared. A bacterial suspension was prepared by inoculating saline solution with 4 – 5 colonies from an overnight culture and agitated to obtain an even turbidity. The OD of the bacterial suspension was measured by using a UV spectrophotometer and adjusted to obtain the density of a 0.5 McFarland turbidity standard (Absorbance: 0.08 – 0.13 at a wavelength of 625 nm). A sterile cotton swab was dipped into the bacterial suspension and used to streak the agar plate three times and after each time rotating the plate at an angle of 60°. The foam samples (cylindrical samples 8 mm in diameter) were placed onto the agar and sealed using parafilm.

The plates were then placed inverted into the incubator and left for 24 hours at 25°C. The inhibition zones were measured using Vernier calipers and recorded.

2.5   Characterization

2.5.1   Staining

Live/dead staining was performed to determine the viability of the *Erwinia carotovora* in the antibacterial foams after the 24-hour experiment. The foams were dissected into four sections and rinsed with water. The water obtained from each section was stained using SYTO9 (Green Stain, Live Bacteria) and propidium iodide (Red Stain, Dead Bacteria). The samples containing the dyes were incubated at room temperature for 15 min under dark conditions. Results were analysed using a fluorescence microscope (EVOS microscope) at ×20 magnification.

2.5.2   Scanning Electron Microscope – Energy Dispersive X-Ray Spectroscopy (SEM-EDX)

A JEOL SEM (JSM-6480LV) instrument was used to analyse the surface of the foam samples, to confirm the presence of live/dead bacteria as well as to determine the distribution of copper and nickel in the antibacterial foams. For the analysis of the foam surface, the samples were mounted onto a stainless-steel sample holder and held in place by using a carbon adhesive. For the confirmation of the death of the bacteria in the foam, the samples were prepared via a bacteria fixing process prior to the SEM session. They were then placed in a vacuum desiccator overnight to remove moisture present in the sample. A Quorum Q150TS instrument was used to coat the foam samples with a thin layer of Chromium prior to the SEM analysis. Samples for EDX analysis were not coated with chromium. They were then mounted onto the sample stage in a small vacuum chamber at room temperature and pressure. An electron beam was projected onto the sample surface and the deflected electrons were detected by an electron sensor. This deflection formed the image of the sample surface and it was recorded by a computer.

3 Results and Discussion

3.1 Fabrication of PI/Copper, PI/Nickel & PI/Copper – Nickel Composite foams

PCu80, PNi80 and PI/copper – nickel composite foams were successfully fabricated by using the method described in Section 2.2. The composition of the foams can be seen in Table 1. PCu80 and PNi80 foams can be seen in Figure 2a,b respectively.
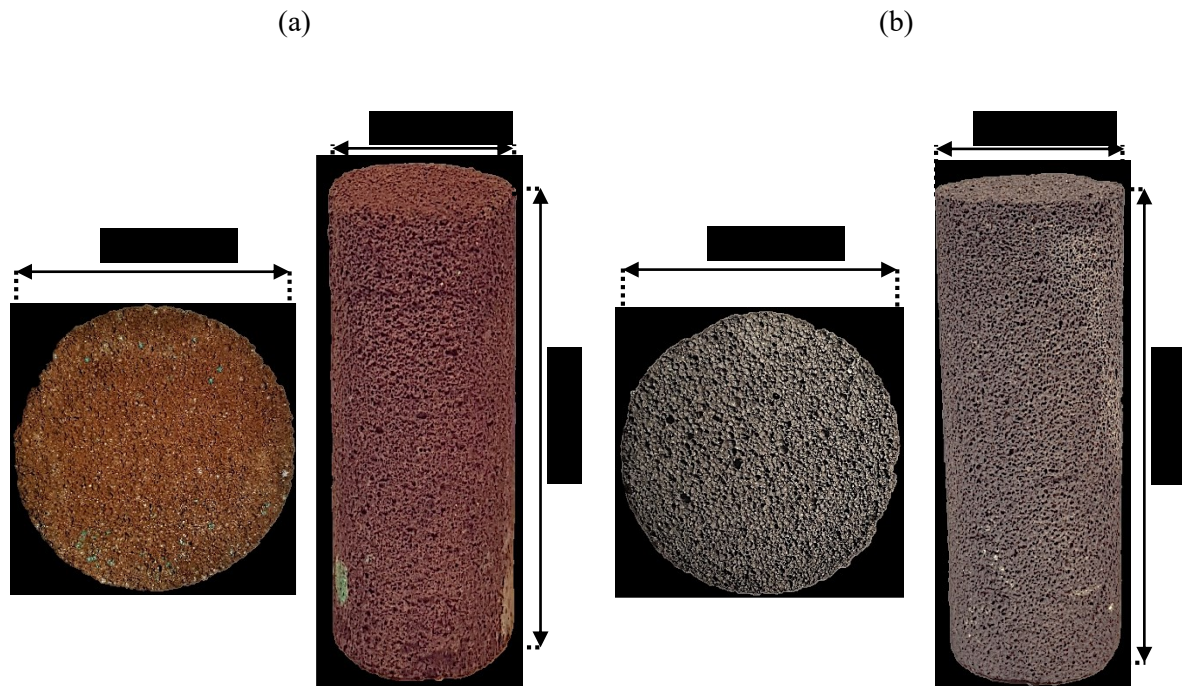
(a)   (b)

Figure 2. Antibacterial polyimide foams with 80 wt% copper (a) PCu80 (top and side – view) and 80 wt% nickel (b) PNi80 (top and side – view), Legend: P indicates polyimide, Cu indicates copper, Ni indicates nickel, 80 indicates weight percentage of antibacterial agent in the foam.

Both PCu80 and PNi80 were similar in terms of dimensions and structure. The most significant difference would be the colour of PCu80 and PNi80 due to the copper and nickel powder used respectively. PCu80 displayed a 'reddish – brown' color whereas PNi80 displayed a 'charcoal – grey' color as shown in Figure 2a,b respectively. Unlike the cross-section of PNi80, small 'blue – green' specks were observed on the cross-section of PCu80. This could be due to the copper undergoing an oxidation process to form copper carbonate in the presence

11

of oxygen, moisture and carbon dioxide during the foaming process as well as in the water bath when the copper foams were soaked overnight. The influence of copper and nickel on the density and porosity of the foams was determined by comparing a polyimide foam (no copper/nickel) with PCu80 and PNi80. The density of the polyimide foam (no copper/nickel) was 203 kg m^{-3} ± 2.7% whilst the densities of both PCu80 and PNi80 were 282 kg m^{-3} ± 4.3% and 248 kg m^{-3} ± 1.1% respectively. The porosity of the polyimide foam (no copper/nickel) was 0.82 ± 1.6% whilst the porosities of both PCu80 and PNi80 were 0.74 ± 4% and 0.76 ± 2.2% respectively. This shows that copper and nickel did not have a significant influence on the density and porosity of the foam. Additionally, there was no considerable influence of the copper and nickel on the rigidity of the foam compared to the polyimide foam (no copper/nickel).

3.2 SEM-EDX Analysis

SEM-EDX analysis was performed on the antibacterial foam samples to confirm the presence of copper – nickel and to ensure an even distribution of the antibacterial material throughout the length of the foam. SEM images of pure copper and nickel powder were first taken to assess the appearance of the particles so that they can be easily detected in their respective foams. This can be seen in Figure 3a,b for the copper (granule-like appearance) and nickel (flake-like appearance) powder respectively. The cross-sections of PCu80 (Figure 3c) and PNi80 (Figure 3d) were taken at a lower magnification to measure the pore-window diameter and pore diameter as identified in Figure 3c. Similar measurements were also performed for a polyimide foam (no copper/nickel) and compared against PCu80 and PNi80. The pore window diameter for the polyimide foam (no copper/nickel) ranged from 309.5 – 690.5 μm whilst the pore window diameter for PCu80 and PNi80 ranged from 388.9 – 925.9 μm and 357.1 – 1119.0 μm respectively. The pore diameter for the polyimide foam (no copper/nickel) ranged from 71.4 – 285.7 μm whilst the pore diameter for PCu80 and PNi80 ranged from 111.1 – 296.3 μm and

71.4 – 261.9 μm respectively. These pore data show that the foam structures are similar in morphology with the presence of mesopores and macropores. In addition, Figure 3c,d show that the PCu80 and PNi80 foams have a similar open cell structure and this was supported by minimal back pressure observed during the antibacterial flow – through experiments performed at 1 L min^{-1}. At a higher magnification of the cross-section of PCu80, particles with a granule-like appearance (Figure 3e) were observed and they were similar to the pure copper powder observed in Figure 3a. As for PNi80, at a higher magnification, particles with a flake-like appearance (Figure 3f) were observed and they were similar to the pure nickel powder in Figure 3b.
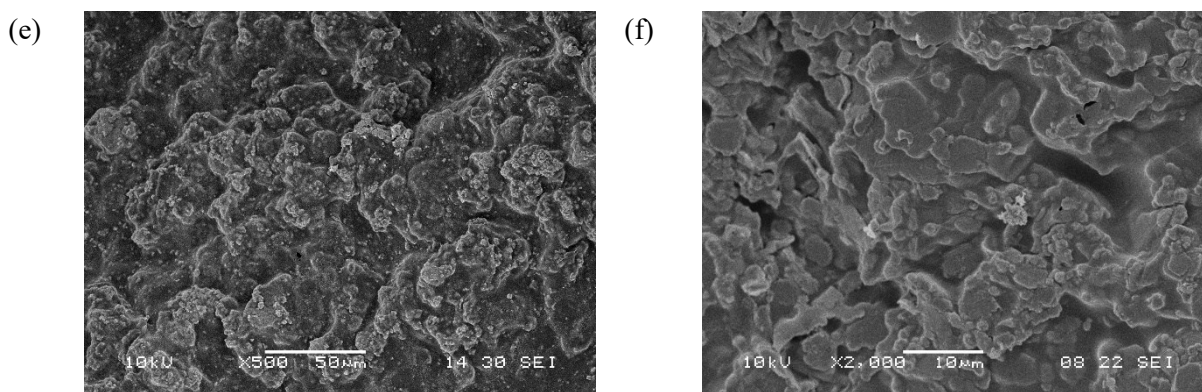
(e) (f)
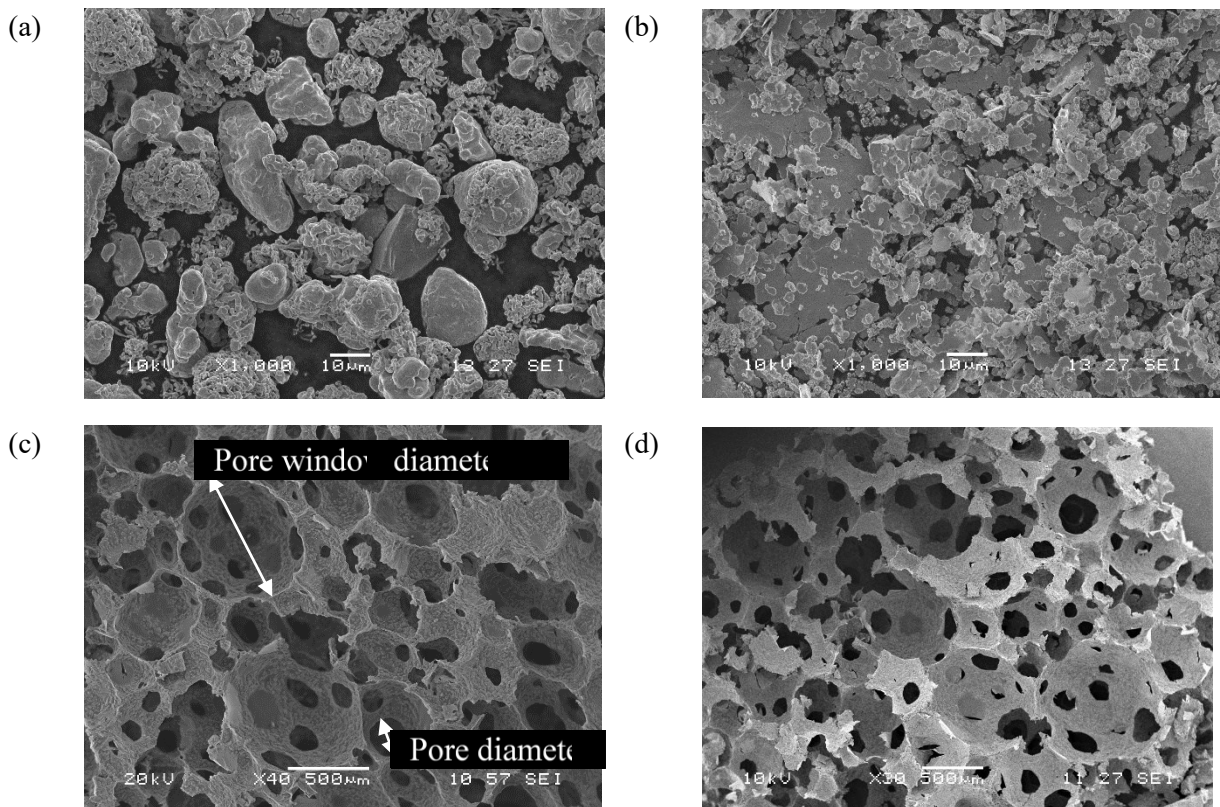
Figure 3. SEM of (a) Pure copper powder (×1,000), (b) Pure nickel powder (×1,000), (c) PCu80 (×40), (d) PNi80 (×30), (e) PCu80 (×500), (f) PNi80 (×2,000), Legend: P indicates polyimide, Cu indicates copper, Ni indicates nickel, 80 indicates weight percentage of antibacterial agent in the foam.

After confirming the presence of copper and nickel in their respective foams, samples were taken from the top, middle and bottom of each foam and analysed by using EDX (Figure 4) to ensure an even distribution of the antibacterial material throughout the length of the foam. As expected, the percentage of copper (Figure 4a,b,c) and nickel (Figure 4d,e,f) detected ranged between 70 – 75% in all cases. Similar percentages of antibacterial material were detected in the top, middle and bottom samples of the foam, thereby indicating that there is a relatively homogenous mixture of the antibacterial agent throughout the length of the foam. Similarly, samples from the top, middle and bottom were taken from PCu64Ni16 (Figure 4g,h,i) and analysed by using EDX to ensure an even distribution of copper : nickel ratios (4 : 1) in the composite foam. The percentage of copper present in all three sections was approximately four times the percentage of nickel which was expected from PCu64Ni16. Although silicon was detected in PCu80, PNi80 and PCu64Ni16, the percentage of silicon present was very low. The presence of silicon may have been due to the remaining residue of the silicon oil that was used during the foaming process. Carbon and oxygen were the next commonly found elements and this was due to the polyimide present in the foam samples.
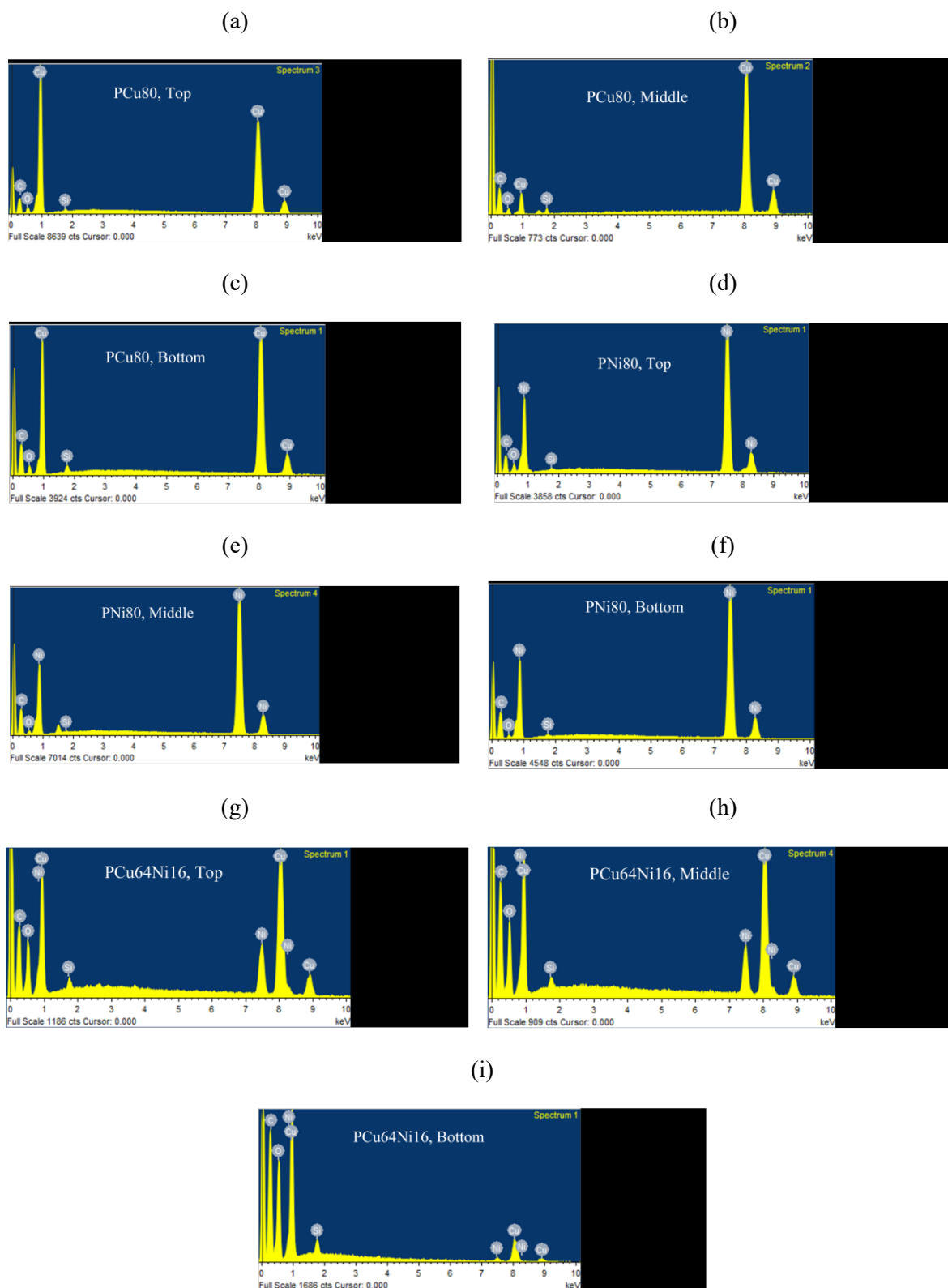
Figure 4. EDX analysis of PCu80 foam sample (a) Top, (b) Middle, (c) Bottom, EDX analysis of PNi80 foam sample (d) Top, (e) Middle, (f) Bottom, EDX analysis of PCu64Ni16 foam

sample (g) Top, (h) Middle, (i) Bottom, Legend: P indicates polyimide, Cu indicates copper, Ni indicates nickel, 80 indicates weight percentage of antibacterial agent in the foam.

3.3   Antibacterial Tests

The efficacy of the antibacterial foams was determined by calculating log reduction values and bacterial death was confirmed by using cell staining and SEMs.

3.3.1   Log Reduction Values (LRVs) for PI/Copper (80 wt%) and PI/Nickel (80 wt%)

Table S1 shows the LRVs achieved when two P-0 (Control, polyimide foam without antibacterial agent), three PCu80 (80 wt% copper) and three PNi80 (80 wt% nickel) foams were tested using Gram-negative *Erwinia carotovora*. The foams have also been re – tested after being sterilised (in bleach solution, autoclaved and dried in oven) and minimal changes were observed in the antibacterial efficacy of the foams. P-0 was analysed prior to PCu80 and PNi80 to find the filtration efficiency of a non-functional foam against bacteria. P-0 was able to achieve and maintain an LRV of 2-Log to 3-Log for 6 hours, before starting to decrease down to 1-Log at 24 hours. Compared to P-0, PCu80 and PNi80 were able to achieve much higher LRV values. This can be seen in Table S1. This shows that in addition to the filtration effect, the effect of introducing antibacterial agents into the foam has further improved the efficacy of the foam as the bacteria are not only trapped but also killed. Therefore, a reduction is observed in the number of bacteria that are released into the environment for an extended period of time. The LRVs for PCu80 and PNi80 showed similar values for 2 hours. After 2 hours, the LRV for PCu80 remained at 5-Log up to the 6-hour time point before dropping back down to 4-Log at 24 hours. Unlike PCu80, the LRVs for PNi80 decreased to 4-Log at 4 hours and remained constant till they eventually dropped to 2-Log at 24 hours. High LRVs were maintained even after 24 hours by PCu80 but a reduction in LRV was observed for PNi80 after 6 hours. This suggests that the antibacterial effect of copper and nickel may differ from each

other. This was further analysed using cell staining and SEMs for the detection of live/dead bacterial cells.

3.3.2 Detection of Live/Dead Cells

Cell staining was performed on both PCu80 and PNi80 using propidium iodide (red stain) and SYTO 9 (green stain). Figure 5a was obtained when P-0 was tested and this was used as a control to compare with the staining images for PCu80 and PNi80. In Figure 5a there were only live bacteria present and similarly in Figure 5c, PNi80 had mostly green (live) stains. Unlike PNi80, in Figure 5b, PCu80 had mostly red (dead) and a few green (live) stains. This shows that nickel did not exhibit bactericidal activity as observed with copper.
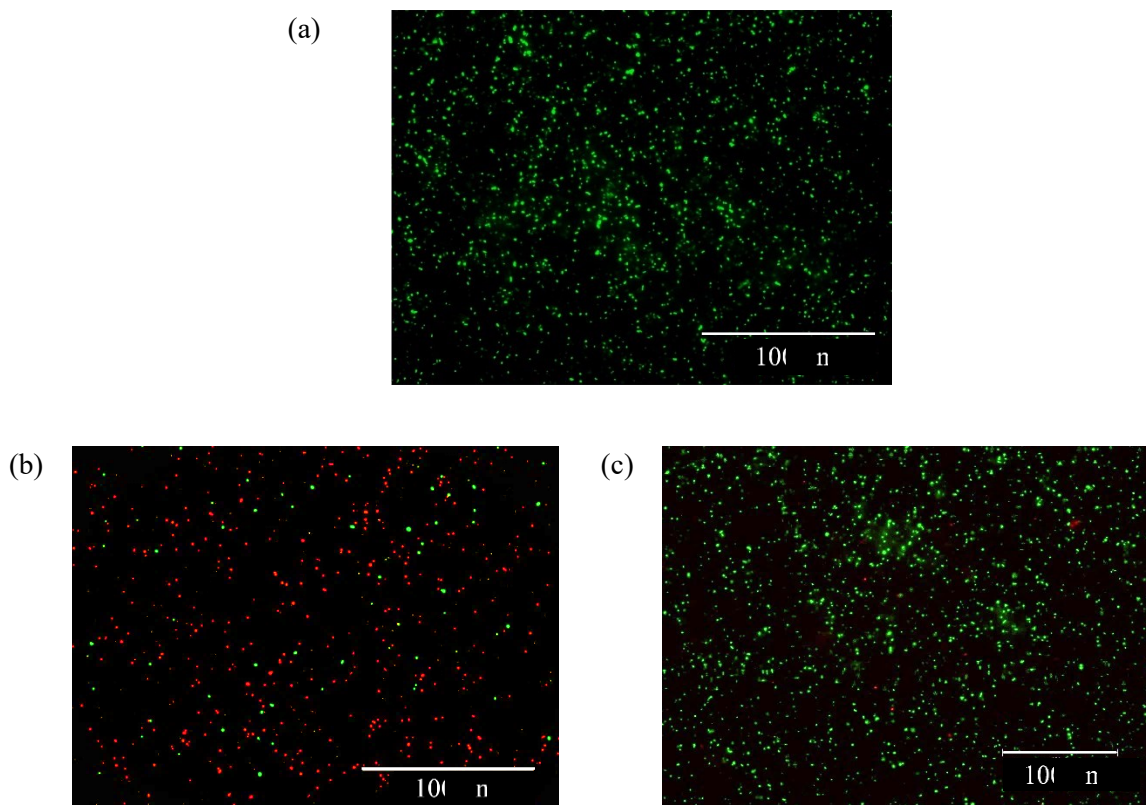

Figure 5. (a) Staining of live bacteria present in P-0 (Control without antibacterial material), Staining of (b) PCu80, (c) PNi80, Legend: P indicates polyimide, Cu indicates copper, Ni indicates nickel, 80 indicates weight percentage of antibacterial agent in the foam.

As the bacterial aerosol passes through PCu80, the bacteria come into contact with the copper particles embedded in the polyimide foam. The cell envelope of a Gram-negative bacteria is comprised of a cytoplasmic membrane (inner) and an outer membrane separated by a peptidoglycan layer.[39] Lipopolysaccharides are negatively charged molecules that are a major component of the outer membrane.[40] As a result of the high moisture content in the aerosol, positively charged copper ions released from the copper particles may have adhered to the negatively charged cell surface and damaged the outer and inner membranes of the bacterial cell.

Therefore, red stain was observed in Figure 5b as the red fluorescent nucleic acid stain propidium iodide can only penetrate cells with disrupted membranes. Although the green fluorescent nucleic acid stain SYTO 9 has the ability to enter both live and dead bacteria cells, in the presence of both propidium iodide and SYTO 9, propidium iodide exhibits a stronger affinity for nucleic acids and thus displaces SYTO 9.[41] Similar results of red-staining were observed by Espirito Santo et al.[42] when *Escherichia coli* cells were exposed to a dry copper surface. Although the pathogenicities of *Escherichia coli* and *Erwinia carotovora* are different, both bacteria are Gram-negative and thus the antibacterial effect of copper on the bacteria would be similar.

Upon damage of the bacterial membrane, the copper ions may have entered the bacterial cell and this was observed by Tian et al.[43] when Gram-negative *Enterobacter* species were exposed to a dry metallic copper surface. The presence of copper ions in the bacterial cell may have caused damage to intracellular components and DNA. In the presence of oxygen, the copper ions undergo redox cycling between Cu^+ and Cu^{2+} oxidation states in the presence of H_2O_2 which is a by-product of oxygen metabolism. This is a Fenton-type reaction which results in the production of reactive oxygen species (ROS) such as hydroxyl radicals.[44] The production of hydroxyl radicals was confirmed by Warnes et al.[45] in *Escherichia coli* cells. These hydroxyl

radicals damage DNA by removing electrons from base moieties as well as adding electrons to unsaturated bases, thereby leading to the formation of lesions in the structure of the DNA strand.[46]

Simultaneously, the alteration in the permeability of the bacterial cell may have resulted in the leakage of the contents in the cell. This can be seen in Figure 6a where the live *Erwinia carotovora* bacteria grown on a polymeric foam (without antibacterial agent) substrate, were long and rod-shaped whereas in Figure 6b, the bacteria appear shrunk, significantly smaller and display a flat or grain-like appearance in a PCu80 foam. Raffi et al.[47] observed similar morphological changes to the *Escherichia coli* cells, which shrunk and changed from a regular rod-shape to an irregular appearance after being treated with copper nanoparticles in liquid growth medium.
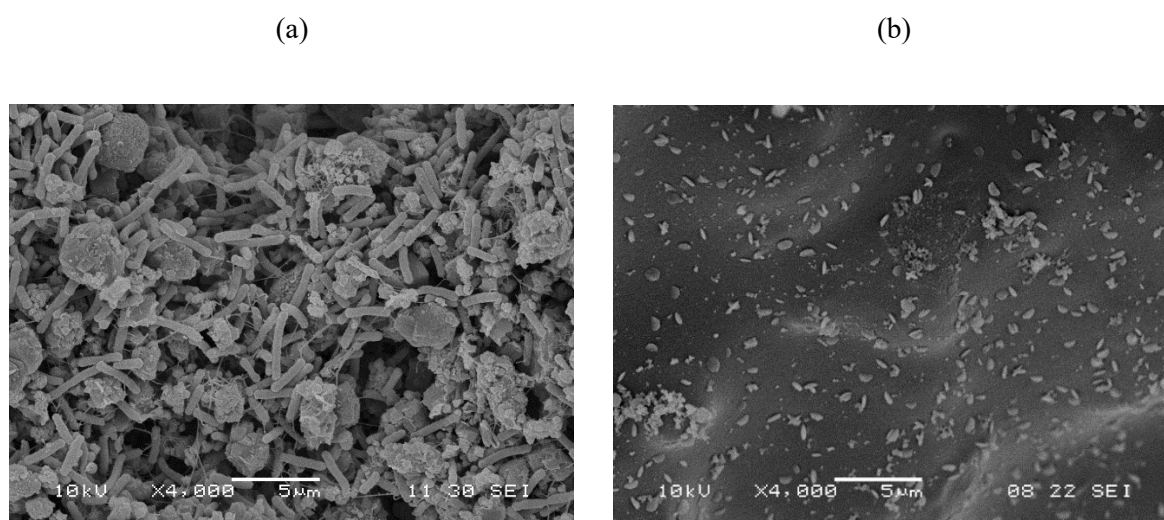
(a)   (b)

Figure 6. (a) SEM of live *Erwinia carotovora* grown on a polymeric foam without antibacterial agent (×4,000), (b) SEM of dead bacteria in PCu80 (PI/copper (80 wt%)) (×4,000).

The lack of red staining in PNi80 (Figure 5c) shows that the cell envelope of the bacteria may have remained intact. However, the LRV at 24 hours for PNi80 was much higher compared to P-0 as shown in Table S1 which suggests that nickel may be exhibiting a bacteriostatic effect where bacterial growth rate is reduced compared to a bactericidal effect

19

observed with copper. This was confirmed by Argueta-Figueroa et al.[18] when nickel nanoparticles were tested against both Gram-positive and Gram-negative bacteria. There is a possibility that the nickel ions may have been able to exhibit the bacteriostatic effect by entering the bacterial cell without disrupting the cell envelope.

Escherichia coli cells were found to have a nickel transport system comprising of proteins: NikA (primary substrate receptor for nickel uptake), NikB and NikC (pore for the translocation of nickel), NikD and NikE (ATP-binding proteins for coupling energy to nickel transport) and NikR (nickel regulatory protein). They have the ability to regulate the concentration of nickel ions that enter the cell so as to avoid the toxic effects of excessive intracellular nickel.[48] However, Niegowski and Eshaghi[49] found that nickel was able to enter *Escherichia coli* cells via CorA proteins which are usually associated with the transport of magnesium ions. CorA proteins are the most dominant and abundant Mg^{2+} transporter in all branches of the bacterial kingdom[50] and these proteins are also present in *Erwinia carotovora* (model bacteria in this work).[33] The nickel ions were still able to gain entry into the *Escherichia coli* cells, even after deleting genes encoding for the Nik A,B,C,D,E,R and CorA proteins.[51] This suggests that the nickel ions may have been able to enter the *Erwinia carotovora* cells without disrupting the cell envelope via CorA and other forms of transporters under high environmental nickel concentrations which explains the lack of red staining observed in Figure 5c.

The replication rate of the *Erwinia carotovora* cells may have been affected by the nickel ions which would explain the reason for lower LRVs to be observed by PNi80 (PI/nickel (80 wt%), Bacteriostatic) compared to PCu80 (PI/copper (80 wt%), Bactericidal), but higher LRVs compared to the control (P-0). Unlike copper, nickel is a poor generator of ROS due to its high redox potential. However, nickel binding to proteins reduces its redox potential and in the presence of H_2O_2, Ni^{2+}/Ni^{3+} redox cycling is initiated. This produces oxygen free radicals which inhibit DNA repair. This was confirmed by Lynn et al.[52] where nickel caused irreversible

damage to proteins involved in DNA replication, repair, recombination and transcription in Chinese hamster ovary cells. However, this was observed in mammalian cells and it may be possible that ROS is not necessary for affecting the rate of replication in bacterial cells. In the absence of ROS, nickel may cause double strand breaks (DSBs) and inhibit the rate of replication due to changes in the DNA topology caused by nickel directly binding to the DNA strand and thus disrupting the function of DNA binding proteins. This was confirmed by Kumar et al.[53] where DNA damage as well as inhibition of DNA repair in *Escherichia coli* cells was observed due to nickel, but in the absence of ROS. The above evidence indicates that regardless of whether it is a mammalian or bacterial cell, the final effect of nickel on DNA does not change.

3.3.3   LRVs for PI/Copper – Nickel Composite Foams

As shown in Table S2, the antibacterial efficacy of the filter can be further improved by using a combination of antibacterial metals. The efficacy of the antibacterial foams containing both copper and nickel was determined by calculating LRVs. As observed in Table S2, the difference in efficacy of the antibacterial foams was more significant at the 24-hr time point. Therefore, the efficacy of the combination foams was presented as a bar chart for only the 24-hr time point as shown in Figure 7.

The LRVs for PCu32Ni48 and PCu48Ni32 were similar to each other for the entire 24 hours and achieved a LRV of 2-Log at the 24-hr time point which was a slight improvement in efficacy compared to PNi80. This can be seen in Table S2 and Figure 7. The minimal improvement in antibacterial efficacy may have been caused by the copper and nickel being present similarly in high percentages in the foam filter. Since both copper and nickel target the DNA, this may have resulted in the antibacterial agents acting on overlapping targets. Argueta-Figueroa et al.[18] also observed that the antibacterial activity of nickel and bimetallic copper-nickel nanoparticles were similar to each other when tested with *Escherichia coli* cells. The

ratio of copper : nickel present in their bimetallic copper-nickel nanoparticles was 1.14 which was slightly lower compared to the ratio of 1.5 (copper : nickel) used in this study.
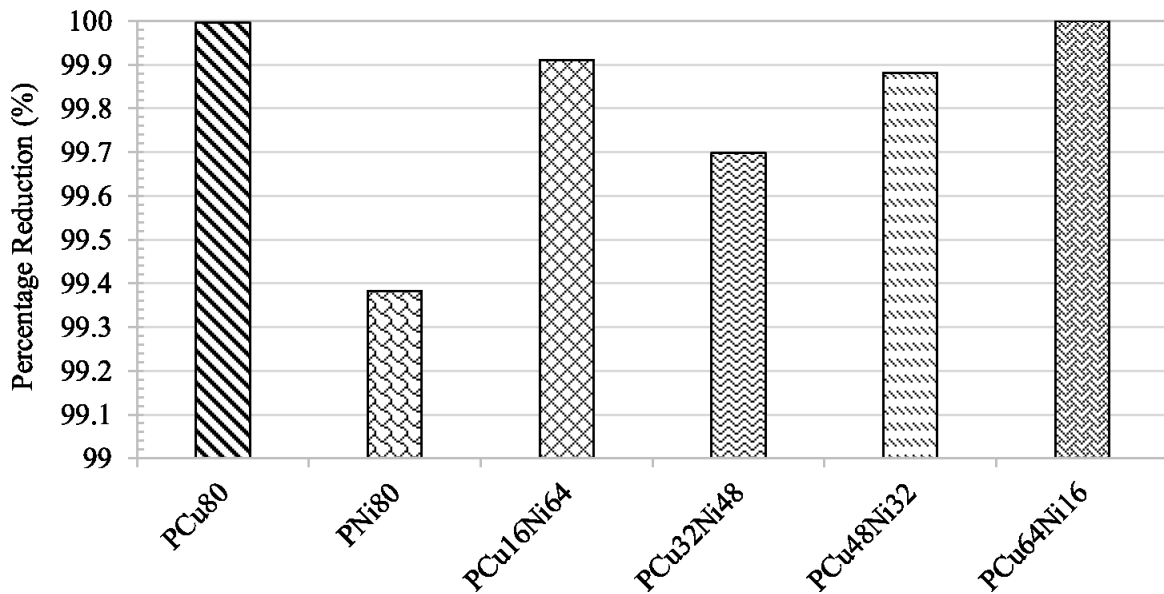

Figure 7. Percentage reduction in bacteria for PI/copper – nickel combination foams at the 24 – hour time point, Legend: P indicates polyimide, Cu indicates copper and Ni indicates nickel.

The percentage of nickel was increased whilst decreasing the percentage of copper (PCu16Ni64). The LRVs for PCu16Ni64 were maintained at 3-log/4-log for 24-hrs and this was an improvement compared to PCu32Ni48. Although PCu16Ni64 performed better than PNi80, it still did not exhibit a higher efficacy compared to Pu80 as shown in Figure 7. It could be possible that higher proportions of nickel present in the filter may have resulted in the bacteriostatic effect to be more dominant compared to the bactericidal effect. As an alternative, the percentage of copper was increased whilst decreasing the percentage of nickel (PCu64Ni16). The LRV for PCu64Ni16 was maintained at 5-log/6-log after 2 hrs and this was a great improvement compared to PCu80. This could be due to the right balance in the percentages of copper and nickel present in the filter. Since copper is able to rupture the bacterial cell envelope, this may have given nickel a quicker entry into the cell compared to

entering the cell via the membrane transporters. Also, the ease at which copper is able to produce hydroxyl radicals compared to nickel may have resulted in DNA damage to take place at an increased rate whilst nickel inhibited DNA repair. This combined effect of bactericidal and bacteriostatic properties may have resulted in cell death to be achieved at an increased rate within the filter and therefore able to maintain high LRVs for a longer period of time.

In support of the LRV data obtained, zone of inhibition tests were also carried out using PCu80, PNi80 and the four PI/copper – nickel composite foams as shown in Figure 8.
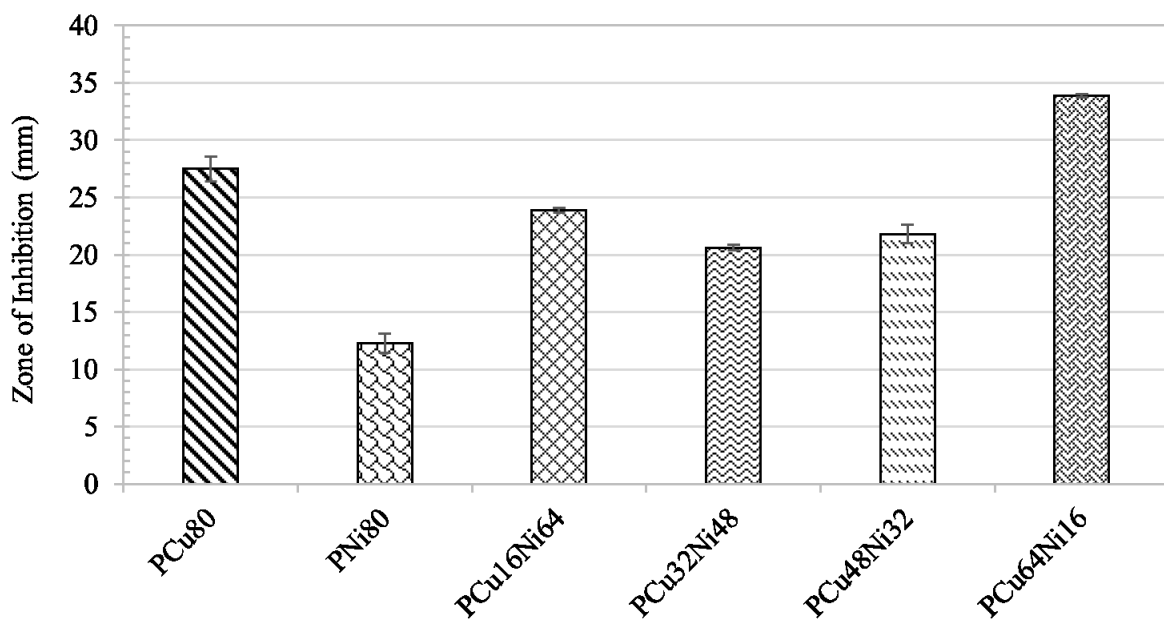

Figure 8. Measurements of zone of inhibition for PCu80 (PI/copper (80 wt%)), PNi80 (PI/nickel (80 wt%)) and PI/copper – nickel composite foams, Legend: P indicates polyimide, Cu indicates copper and Ni indicates nickel, (Reproducibility, n = 3).

Similar to the trend observed in Figure 7, Figure 8 shows that the four PI/copper – nickel composite foams had much higher values of ZOI compared to PNi80 (12.3 ± 0.9 mm). Except for PCu64Ni16 (33.9 ± 0.16 mm), the remaining three [(PCu16Ni64), (PCu32Ni48), (PCu48Ni32)] composite foams exhibited ZOI values of 23.9 ± 0.2 mm, 20.6 ± 0.2 mm and

21.8 ± 0.8 mm respectively and these values were lower than the 27.5 ± 1.1 mm that was observed for PCu80.

The results of the antibacterial tests show that a non-functional PI foam exhibits only a filtration effect due to the porous nature of the foam. However, by including antibacterial agents, the efficacy of the foams is further improved due to the combined effect of filtration provided by the polyimide foam and the individual antibacterial activities of copper and nickel. The combined effect of bactericidal copper and bacteriostatic nickel showed a greater antibacterial efficacy compared to a pure copper foam. Therefore, it could be possible to utilize a combination of different antibacterial agents to improve the antibacterial efficacy of a functionalized foam filter.

4   Conclusions

The antibacterial active polyimide (PI), PCu80 (PI (20 wt%)/copper (80 wt%)) and PNi80 (PI (20 wt%)/nickel (80 wt%)) were successfully prepared via a foaming process comprised of a 'blowing' (CO_2 generation) and polymerization reaction that occurs simultaneously. The antibacterial activity of the foams containing copper, nickel and composite copper – nickel agents were successfully tested against a model Gram-negative bacterium, *Erwinia carotovora*. Copper and nickel concentrations were detected using a Scanning Electron Microscope – Energy Dispersive X-Ray Spectroscopy (SEM – EDX) in PCu80 and PNi80, and it ranged between 70 – 75% and both metals were found to be well distributed throughout the foam indicating that using this one step method, it is possible to manufacture antibacterial foams for flow systems successfully. The concentration of copper in PCu64Ni16 (PI (20 wt%)/copper (64 wt%)/nickel (16 wt%)) was found to be approximately four times the concentration of nickel throughout the foam.

Cell viability was confirmed via SEM and by staining the bacterial cells using a propidium iodide (red stain, dead bacteria) and SYTO 9 (green stain, live bacteria). Antibacterial efficacy of the foam filter was further improved with a copper – nickel composite, PCu64Ni16, which performed far superior than PCu80 due to the combined effect of the bactericidal activity displayed by copper and the bacteriostatic activity displayed by nickel. PCu64Ni16 also exhibited a higher zone of inhibition (ZOI) value than PCu80. These findings show that PI/copper – nickel composite foams can be used for removing microbes from the enclosed space environments by ensuring that they are killed during filtration.

Supporting Information

Log reduction values (%) obtained using P-0, PCu80 and PNi80, Log reduction values (%) for PI/copper – nickel composite foams

Author Information

Corresponding Author

*Email: Semali Perera (cessp@bath.ac.uk); Ramya G (rg377@bath.ac.uk)

Author Contributions

The manuscript was written through contributions of all authors. All authors have given approval to the final version of the manuscript. All authors contributed equally.

Acknowledgements

Abbreviations

DSBs, Double Strand Breaks; DNA, Deoxyribonucleic acid; EUCAST, European Committee of Antimicrobial Susceptibility Testing; HEPA, High-Efficiency Particulate Air; HVAC, Heating, Ventilation and Air-Conditioning; LRVs, Log Reduction Values; NIOSH, National Institute for Occupational Safety and Health; NMP, 1-methyl-2-pyrrolidone; OD, Optical Density; PI, Polyimide; PMDA, Pyromellitic Dianhydride; ROS, Reactive Oxygen Species; SEM-EDX, Scanning Electron Microscope – Energy Dispersive X-Ray Spectroscopy; UV, Ultraviolet; ZOI, Zone of Inhibition.

References

(1)   Decker, H. M.; Buchanan, L.; Goddard, B. S. Air Filtration of Microbial Particles. *Am J Public Heal. Nations Heal.* **1963**, *53* (12), 1982–1988. https://doi.org/10.2105/AJPH.53.12.1982.

(2)   Bernstein, J. A.; Alexis, N.; Bacchus, H.; Bernstein, I. L.; Fritz, P.; Horner, E.; Li, N.; Mason, S.; Nel, A.; Oullette, J.; Reijula, K.; Reponen, T.; Seltzer, J.; Smith, A.; Tarlo, S. M. The Health Effects of Nonindustrial Indoor Air Pollution. *J. Allergy Clin. Immunol.* **2008**, *121* (3), 585–591. https://doi.org/10.1016/j.jaci.2007.10.045.

(3)   Bull, K. Cabin Air Filtration: Helping to Protect Occupants from Infectious Diseases. *Travel Med. Infect. Dis.* **2008**, *6* (3), 142–144. https://doi.org/10.1016/j.tmaid.2007.08.004.

(4)   Menzies, D. Microbial Contamination in Airplane Cabin: Health Effects and Remediation. In *Air Quality in Airplane Cabins and Similar Enclosed Spaces*; Hocking, Martin B.; Hocking, D., Ed.; Springer: Germany, 2005; pp 151–167.

(5)   Möritz, M.; Peters, H.; Nipko, B.; Rüden, H. Capability of Air Filters to Retain Airborne Bacteria and Molds in Heating, Ventilating and Air-Conditioning (HVAC) Systems. *Int. J. Hyg. Environ. Health* **2001**, *203* (5–6), 401–409. https://doi.org/10.1078/1438-4639-00054.

(6)   Maus, R.; Goppelsröder, A.; Umhauer, H. Survival of Bacterial and Mold Spores in Air Filter Media. *Atmos. Environ.* **2001**, *35* (1), 105–113. https://doi.org/10.1016/S1352-2310(00)00280-6.

(7)   Price, D. L.; Simmons, R. B.; Crow, S. A.; Ahearn, D. G. Mold Colonization during Use of Preservative-Treated and Untreated Air Filters, Including HEPA Filters from Hospitals and Commercial Locations over an 8-Year Period (1996-2003). *J. Ind. Microbiol. Biotechnol.* **2005**, *32* (7), 319–321. https://doi.org/10.1007/s10295-005-0226-1.

(8)   Crandall, M. S.; Sieber, W. K. The National Institute for Occupational Safety and Health Indoor Environmental Evaluation Experience. Part One: Building Environmental Evaluations. *Appl. Occup. Environ. Hyg.* **1996**, *11* (6), 533–539. https://doi.org/10.1080/1047322X.1996.10389370.

(9)   Lemire, J. A.; Harrison, J. J.; Turner, R. J. Antimicrobial Activity of Metals:

Mechanisms, Molecular Targets and Applications. *Nat. Rev. Microbiol.* **2013**, *11* (6), 371–384. https://doi.org/10.1038/nrmicro3028.

(10) Santo, C. E.; Quaranta, D.; Grass, G. Antimicrobial Metallic Copper Surfaces Kill Staphylococcus Haemolyticus via Membrane Damage. *Microbiologyopen* **2012**, *1* (2), 46–52. https://doi.org/10.1002/mbo3.2.

(11) Rai, M.; Yadav, A.; Gade, A. Silver Nanoparticles as a New Generation of Antimicrobials. *Biotechnol. Adv.* **2009**, *27* (1), 76–83. https://doi.org/10.1016/j.biotechadv.2008.09.002.

(12) Turner, R. J. Metal-Based Antimicrobial Strategies. *Microb. Biotechnol.* **2017**, *10* (5), 1062–1065. https://doi.org/10.1111/1751-7915.12785.

(13) Vincent, M.; Hartemann, P.; Engels-Deutsch, M. Antimicrobial Applications of Copper. *Int. J. Hyg. Environ. Health* **2016**, *219* (7), 585–591. https://doi.org/10.1016/j.ijheh.2016.06.003.

(14) Villapun, V. M.; Dover, L. G.; Cross, A.; Gonzalez, S. Antibacterial Metallic Touch Surfaces. *Materials (Basel).* **2016**, *9* (9), 1–23. https://doi.org/10.3390/ma9090736.

(15) Michels, H. T.; Noyce, J. O.; Keevil, C. W. Effects of Temperature and Humidity on the Efficacy of Methicillin- Resistant Staphylococcus Aureus Challenged Antimicrobial Materials Containing Silver and Copper. *Lett. Appl. Microbiol.* **2009**, *49* (2), 191–195. https://doi.org/10.1111/j.1472-765X.2009.02637.x.

(16) Vaidya, M. Y.; McBain, A. J.; Butler, J. A.; Banks, C. E.; Whitehead, K. A. Antimicrobial Efficacy and Synergy of Metal Ions against Enterococcus Faecium, Klebsiella Pneumoniae and Acinetobacter Baumannii in Planktonic and Biofilm

Phenotypes. *Sci. Rep.* **2017**, *7* (1), 1–9. https://doi.org/10.1038/s41598-017-05976-9.

(17)   Garza-Cervantes, J. A.; Chávez-Reyes, A.; Castillo, E. C.; García-Rivas, G.; Ortega-Rivera, O. A.; Salinas, E.; Ortiz-Martínez, M.; Gómez-Flores, S. L.; Peña-Martínez, J. A.; Pepi-Molina, A.; Treviño-González, M. T.; Zarate, X.; Cantú-Cárdenas, M. E.; Escarcega-Gonzalez, C. E.; Morones-Ramírez, J. R. Synergistic Antimicrobial Effects of Silver/Transition-Metal Combinatorial Treatments. *Sci. Rep.* **2017**, *7* (1), 1–16. https://doi.org/10.1038/s41598-017-01017-7.

(18)   Argueta-Figueroa, L.; Morales-Luckie, R. A.; Scougall-Vilchis, R. J.; Olea-Mejía, O. F. Synthesis, Characterization and Antibacterial Activity of Copper, Nickel and Bimetallic Cu-Ni Nanoparticles for Potential Use in Dental Materials. *Prog. Nat. Sci. Mater. Int.* **2014**, *24* (4), 321–328. https://doi.org/10.1016/j.pnsc.2014.07.002.

(19)   Vukčević, M.; Kalijadis, A.; Dimitrijević-Branković, S.; Laušević, Z.; Laušević, M. Surface Characteristics and Antibacterial Activity of a Silver-Doped Carbon Monolith. *Sci. Technol. Adv. Mater.* **2008**, *9* (1), 1–7. https://doi.org/10.1088/1468-6996/9/1/015006.

(20)   Lv, D.; Zhu, M.; Jiang, Z.; Jiang, S.; Zhang, Q.; Xiong, R.; Huang, C. Green Electrospun Nanofibers and Their Application in Air Filtration. *Macromol. Mater. Eng.* **2018**, *303* (12), 1–18. https://doi.org/10.1002/mame.201800336.

(21)   Zhu, M.; Hua, D.; Zhong, M.; Zhang, L.; Wang, F.; Gao, B.; Xiong, R.; Huang, C. Antibacterial and Effective Air Filtration Membranes by "Green" Electrospinning and Citric Acid Crosslinking. *Colloids Interface Sci. Commun.* **2018**, *23*, 52–58. https://doi.org/10.1016/j.colcom.2018.01.002.

(22)   Lv, D.; Wang, R.; Tang, G.; Mou, Z.; Lei, J.; Han, J.; De Smedt, S.; Xiong, R.; Huang,

C. Ecofriendly Electrospun Membranes Loaded with Visible-Light-Responding Nanoparticles for Multifunctional Usages: Highly Efficient Air Filtration, Dye Scavenging, and Bactericidal Activity. *ACS Appl. Mater. Interfaces* **2019**, *11* (13), 12880–12889. https://doi.org/10.1021/acsami.9b01508.

(23) Paladini, F.; Cooper, I. R.; Pollini, M. Development of Antibacterial and Antifungal Silver-Coated Polyurethane Foams as Air Filtration Units for the Prevention of Respiratory Diseases. *J. Appl. Microbiol.* **2014**, *116* (3), 710–717. https://doi.org/10.1111/jam.12402.

(24) Hu, J.; Zhong, Z.; Zhang, F.; Xing, W.; Low, Z. X.; Fan, Y. Coating of ZnO Nanoparticles onto the Inner Pore Channel Surface of SiC Foam to Fabricate a Novel Antibacterial Air Filter Material. *Ceram. Int.* **2015**, *41* (5), 7080–7090. https://doi.org/10.1016/j.ceramint.2015.02.016.

(25) Kim, H. S.; Moorcroft, C. I.; McIntyre, A. Flexible Polyurethane Foam Containing Copper. US6387973B1, 2002.

(26) Liu, P.; Chen, G.-F. Applications of Porous Ceramics. In *Porous Materials: Processing and Applications*; Elsevier Ltd: United Kingdom, 2014; pp 341–342.

(27) Montanaro, L.; Jorand, Y.; Fantozzi, G.; Negro, A. Ceramic Foams by Powder Processing. *J. Eur. Ceram. Soc.* **1998**, *18* (9), 1339–1350.

(28) Drioli, E.; Giorno, L. Basic Aspects of Polymeric and Inorganic Membrane Preparation. In *Comprehensive Membrane Science and Engineering*; 2010; p 228.

(29) Vazquez, J. M.; Cano, R. J.; Jensen, B. J.; Weiser, E. S. Polyimide Foams. US7541388B2, 2004.

(30) Takekoshi, T. Synthesis of Polyimides. In *Polyimides: Fundamentals and Applications*; 1996; pp 7–49.

(31) Marvel, C. S. Thermally Stable Polymers. *Pure Appl. Chem.* **1968**, *16* (2–3), 351–368.

(32) Bell, K. S.; Sebaihia, M.; Pritchard, L.; Holden, M. T. G.; Hyman, L. J.; Holeva, M. C.; Thomson, N. R.; Bentley, S. D.; Churcher, L. J. C.; Mungall, K.; Atkin, R.; Bason, N.; Brooks, K.; Chillingworth, T.; Clark, K.; Doggett, J.; Fraser, A.; Hance, Z.; Hauser, H.; Toth, I. K. Genome Sequence of the Enterobacterial Phytopathogen Erwinia Carotovora Subsp. Atroseptica and Characterization of Virulence Factors. *Proc. Natl. Acad. Sci. U. S. A.* **2004**, *101* (30), 11105–11110. https://doi.org/10.1073/pnas.0402424101.

(33) Kersey, C. M.; Agyemang, P. A.; Dumenyo, C. K. CorA, the Magnesium/Nickel/Cobalt Transporter, Affects Virulence and Extracellular Enzyme Production in the Soft Rot Pathogen Pectobacterium Carotovorum. *Mol. Plant Pathol.* **2012**, *13* (1), 58–71. https://doi.org/10.1111/j.1364-3703.2011.00726.x.

(34) Byers, J. T.; Lucas, C.; Salmond, G. P. C.; Welch, M. Nonenzymatic Turnover of an Erwinia Carotovora Quorum-Sensing Signaling Molecule. *J. Bacteriol.* **2002**, *184* (4), 1163–1171. https://doi.org/10.1128/JB.184.4.1163.

(35) G, R.; Crittenden, B.; Smith, M.; Camus, O.; Chew, Y. M. J.; Perera, S. Synthesis of Novel Regenerable 13X Zeolite-Polyimide Adsorbent Foams. *Chem. Eng. J.* **2019**, *361*, 736–750. https://doi.org/10.1016/j.cej.2018.12.096.

(36) Safiuddin, M.; Hearn, N. Comparison of ASTM Saturation Techniques for Measuring the Permeable Porosity of Concrete. *Cem. Concr. Res.* **2005**, *35* (5), 1008–1013.

(37) BSI Standards Publication. *Measurement of Antibacterial Activity on Plastics and Other*

Non-Porous Surfaces; 2011. https://doi.org/10.1017/CBO9781107415324.004.

(38)   EUCAST. *Antimicrobial Susceptibility Testing EUCAST Disk Diffusion Method - Version 7.0*; 2019.

(39)   Silhavy, T. J.; Kahne, D.; Walker, S. The Bacterial Cell Envelope. *Cold Spring Harb Perspect Biol* **2010**, *2*, 1–16. https://doi.org/10.1101/cshperspect.a000414.

(40)   Rosenfeld, Y.; Shai, Y. Lipopolysaccharide (Endotoxin)-Host Defense Antibacterial Peptides Interactions: Role in Bacterial Resistance and Prevention of Sepsis. *Biochim. Biophys. Acta - Biomembr.* **2006**, *1758* (9), 1513–1522. https://doi.org/10.1016/j.bbamem.2006.05.017.

(41)   Stocks, S. M. Mechanism and Use of the Commercially Available Viability Stain, BacLight. *Cytom. Part A* **2004**, *61* (2), 189–195. https://doi.org/10.1002/cyto.a.20069.

(42)   Santo, C. E.; Lam, E. W.; Elowsky, C. G.; Quaranta, D.; Domaille, D. W.; Chang, C. J.; Grass, G. Bacterial Killing by Dry Metallic Copper Surfaces. *Appl. Environ. Microbiol.* **2011**, *77* (3), 794–802. https://doi.org/10.1128/AEM.01599-10.

(43)   Tian, W. X.; Yu, S.; Ibrahim, M.; Almonaofy, A. W.; He, L.; Hui, Q.; Bo, Z.; Li, B.; Xie, G. lin. Copper as an Antimicrobial Agent against Opportunistic Pathogenic and Multidrug Resistant Enterobacter Bacteria. *J. Microbiol.* **2012**, *50* (4), 586–593. https://doi.org/10.1007/s12275-012-2067-8.

(44)   Pham, A. N.; Xing, G.; Miller, C. J.; Waite, T. D. Fenton-like Copper Redox Chemistry Revisited: Hydrogen Peroxide and Superoxide Mediation of Copper-Catalyzed Oxidant Production. *J. Catal.* **2013**, *301*, 54–64. https://doi.org/10.1016/j.jcat.2013.01.025.

(45)   Warnes, S. L.; Caves, V.; Keevil, C. W. Mechanism of Copper Surface Toxicity in

Escherichia Coli O157:H7 and Salmonella Involves Immediate Membrane Depolarization Followed by Slower Rate of DNA Destruction Which Differs from That Observed for Gram-Positive Bacteria. *Environ. Microbiol.* **2012**, *14* (7), 1730–1743. https://doi.org/10.1111/j.1462-2920.2011.02677.x.

(46) Imlay, J. A. Pathways of Oxidative Damage. *Annu. Rev. Microbiol.* **2003**, *57* (1), 395–418. https://doi.org/10.1146/annurev.micro.57.030502.090938.

(47) Raffi, M.; Mehrwan, S.; Bhatti, T. M.; Akhter, J. I.; Hameed, A.; Yawar, W.; Ul Hasan, M. M. Investigations into the Antibacterial Behavior of Copper Nanoparticles against Escherichia Coli. *Ann. Microbiol.* **2010**, *60* (1), 75–80. https://doi.org/10.1007/s13213-010-0015-6.

(48) Eitinger, T.; Mandrand-Berthelot, M. A. Nickel Transport Systems in Microorganisms. *Arch. Microbiol.* **2000**, *173* (1), 1–9. https://doi.org/10.1007/s002030050001.

(49) Niegowski, D.; Eshaghi, S. The CorA Family: Structure and Function Revisited. *Cell. Mol. Life Sci.* **2007**, *64* (19–20), 2564–2574. https://doi.org/10.1007/s00018-007-7174-z.

(50) Moncrief, M. B. C.; Maguire, M. E. Magnesium Transport in Prokaryotes. *J. Biol. Inorg. Chem.* **1999**, *4* (5), 523–527. https://doi.org/10.1007/s007750050374.

(51) MacOmber, L.; Hausinger, R. P. Mechanisms of Nickel Toxicity in Microorganisms. *Metallomics* **2011**, *3* (11), 1153–1162. https://doi.org/10.1039/c1mt00063b.

(52) Lynn, S.; Yew, F. H.; Chen, K. S.; Jan, K. Y. Reactive Oxygen Species Are Involved in Nickel Inhibition of DNA Repair. *Environ. Mol. Mutagen.* **1997**, *29* (2), 208–216. https://doi.org/10.1002/(SICI)1098-2280(1997)29:2<208::AID-EM11>3.0.CO;2-I.

(53) Kumar, V.; Mishra, R. K.; Kaur, G.; Dutta, D. Cobalt and Nickel Impair DNA Metabolism by the Oxidative Stress Independent Pathway. *Metallomics* **2017**, *9* (11), 1596–1609. https://doi.org/10.1039/c7mt00231a.